Development of Targeted Therapy Therapeutics to Sensitize Triple-Negative Breast Cancer Chemosensitivity Utilizing Bacteriophage phi29 Derived Packaging RNA

Long Zhang
Wenzhou Medical University
Chaofeng Mu
Zhejiang Chinese Medical University
Tinghong Zhang (zhangth@wiucas.ac.cn)
Wenzhou Medical University
Dejun Yang
Wenzhou Medical University
Luhui Fan
Zhejiang Chinese Medical University
Cong Liu
Zhejiang Chinese Medical University
Chenou Wang
Wenzhou Medical University
Qiong Chen
Wenzhou Medical University
Jianliang Shen
Wenzhou Medical University
Huaqiong Li
Wenzhou Institute of Biomaterials and Engineering https://orcid.org/0000-0002-6151-6479

Research

Keywords: RNA nanoparticles, XBP1, siRNA, TNBC, Chemoresistance

Posted Date: August 7th, 2020

DOI: https://doi.org/10.21203/rs.3.rs-51875/v1

Version of Record: A version of this preprint was published on January 7th, 2021. See the published version at https://doi.org/10.1186/s12951-020-00758-4.

Abstract

Background: To date, triple-negative breast cancer (TNBC) treatment options are limited due to it lacks expression of receptors and are only available managed with chemotherapy. What's worse, TNBC is frequently developing resistance to chemotherapy. By using siRNA-based therapeutics, our recent work demonstrated X-box-binding protein 1 (XBP1) was linked to HER2+ breast cancer development and chemoresistance. As is well-known, the instability, off-target effects, net negative charge, and hydrophobicity of siRNA hamper its' *in vivo* utilization and clinical transformation. Thus, the development of a siRNA delivery system (DDS) with ultra-stability and specificity is demanded to address the predicament of siRNA delivery.

Results: Here, we assembled RNase resistant RNA nanoparticles (NPs) based on the 3WJ of Phi29 DNA packaging motor. To targeted therapy and sensitize TNBC to chemotherapy, the RNA NPs were equipped with epidermal growth factor receptor (EGFR) targeting aptamer and XBP1 siRNA. We found our RNA NPs could deplete XBP1 expression and suppress tumor growth after intravenous administration. Meanwhile, RNA NPs treatment could promote the sensitization of chemotherapy and impair angiogenesis *in vivo*.

Conclusions: The results further demonstrate that our RNA NPs could serve as an effective and promising platform not only for siRNA delivery but also for chemotherapy-resistant TNBC therapy.

Background

TNBC, which accounts for 12% to 18% of breast cancer patients, is a more aggressive subtype of breast cancer with poor prognosis and overall survival (OS) [1]. TNBC is negative for estrogen, progesterone, and human epidermal growth factor receptor 2 (HER2) receptor and therefore is not eligible for target therapy. Anthracyclines (doxorubicin et al.) and taxanes (paclitaxel et al.) based neoadjuvant chemotherapy (NAC) is the standard therapy method to manage TNBC [2]. However, due to chromosomal instability, about 50% NAC treated patients evolve chemoresistance [3]. Our recent results showed XBP1 involves in HER2+ breast cancer development and chemoresistance [4]. XBP1 was also reported regulates a HIF1α-dependent transcriptional network in TNBC cells, which facilitates TNBC progression and chemoresistance [5]. Meanwhile, XBP1 expression shows a positive correlation with cell survival of TNBC [6, 7]. However, related effective and promising drugs target both TNBC and XBP1 to sensitize TNBC to chemotherapy is still no explored.

siRNA is widely used to probing gene function by targeting specificity mRNA expression and against various diseases. In November 2019 the second siRNA-based drug has been approved by the FDA, which represents a landmark event for the advancement of RNA-based medicines [8]. However, due to its instability, net negative charge, and hydrophobicity and, *in vivo* utilization of siRNA remains a major challenge [9]. Over the past 20 years, the novel siRNA DDS developed rapidly, including cationic polymer-based [10], exosome-based [11], membrane-camouflage [12], lipid-based [13], and nanogel-based [14]. Unfortunately, present DDS possess unique drawbacks (such as large particle size, cytotoxicity,

aggregation *in vivo,* and immune response), which impedes *in vivo* application [15-17]. Recently, we proved that using phi29 bacteriophage-derived pRNA could deliver siRNA with high-efficiency [4]. The RNA nanotechnology was developed in 1998 [18] and has been widely used in cancer therapy [19-21]. Compare to other DDS, this pRNA nanoparticle' branched ratchet shape, and favorable sizes (about 10 nm) facilitates tumor penetration [22, 23]. The RNA NPs equip with tumor targeting aptamer can ensure NPs bind to tumor cells with little in healthy organs [24, 25]. At the same time, its electronegativity prevents nonspecific cell targeting, which results in minimum cytotoxicity and off-target effects [26]. Excitingly, chemical modifications of RNA bases can confer RNA NPs more stability to against serum and RNase [27]. At last, RNA NPs were composed with RNA that is easy to synthesize and minimal induction of adverse immune response [28].

In this study, we set out to target therapy TNBC and sensitize TNBC to chemotherapy by using RNA nanotechnology. We found that after intravenous injections of macromolecular pRNA NPs dramatically suppressed breast cancer growth and promoted the sensitization of chemotherapy in TNBC mouse model. XBP1 deletion impaired angiogenesis and combined treatment with RNA NPs and doxorubicin (dox) can further impaired angiogenesis and down-regulated HIF1α target expressions. Our findings imply that macromolecular pRNA platform could efficiently deliver similarly macromolecular siRNA. This may offer an effective and promising way for chemotherapy resistant TNBC treatment in the future.

Materials And Methods

Cell culture

Breast cancer cell lines MDA-MB-231 and MDA-MB-453 and normal mammary epithelial cells MCF-10A, 184B5 cells were purchased from Chinese Academy of Sciences Cell Bank (Shanghai, China).

MDA-MB-231, MDA-MB-453 were cultured in Leibovitz's L-15 medium (Gibco) supplemented with 100 units/mL penicillin streptomycin, 10% FBS (Gibco) and kept at 37 ^{o}C in humidified 100% atmosphere. 184B5 cells were cultured in DMEM (Gibco) supplemented with 10% FBS and antibiotics and kept at 37 ^{o}C, 5% CO_2. MCF10A cells were cultured in MEGM (Lonza) supplemented with 100 ng/mL cholera toxin, supplements and growth factors (Lonza) (BPE, hEGF, Insulin, Hydrocortisone, GA-1000), and kept at 37 ^{o}C, 5% CO_2.

Generation of 3WJ-EGFRapt-siXBP1 NPs

Multifunctional pRNA-EGFRapt-siXBP1NPs were driven from ph29 pRNA and constructed using a bottom-up self-assembly approach [29].

The therapeutic pRNA-EGFRapt-siXBP1 is composed of four strands. Lowercase letters indicate 2'-F modified nucleotides, and other sequences are adopted as previously described [4].

Strand 1: 5'-uucuuucGAucucuGGcAGuu-3’;

Strand 2: 5'-cuGccAGAGAucGAAAGAAuuuuGccAuGuGuAuGuGGG-3';

Strand 3: 5'-ccc AcA uAc uuu Guu GAu ccG ccu uAG uAA

cGu Gcu uuG AuG ucG Auu cGA cAG GAG Gc-3' (underlined sequence is EGFR aptamer) [30];

Strand 4: 5'-GGAucAAucAuGGcAA(Cy5)-3'.

The control pRNA-EGFRapt-siScramble is composed of strands with siScramble sequence instead of siXBP1 sequence. Lowercase letters indicate 2'-F modified nucleotides. The siScramble sequence is as follows:

Sense: 5'-GccAGAAAcGGuAcAAGuA-3';

Antisense: 5'-uAcuuGuAccGuuucuGGc-3'.

Characterization of pRNA-EGFRapt-siXBP1 NPs

The size and zeta potential of our NPs were determined by DLS. The Tm value was detected by a SYBR green assay, as previously described [4]. For stability assay, the 2'F modified NPs or unmodified 3WJ control NPs were exposed to different concentrations RNase A (0, 10, 100 μg/mL), or 10% FBS supplemented DMEM medium at 37 ^{o}C, respectively. The assembly and stability of our NPs was examined through 8% native PAGE gel electrophoresis.

In vitro cell binding and uptake

Flow cytometry and confocal microscope were used to evaluate the cellular binding and uptake of NPs. To do this, MDA-MB-231 cells were grown on slides overnight in L15 medium and incubated with 50 nM Cy5-conjugated NPs for 24 h at 37 ^{o}C. After washing three times with pre-cooling PBS, cells were fixed and stained with cytomembrane dye Alexa488-wheat germ agglutinin (Thermo Fisher) and DAPI (Sigma). The slides were imaging using a Nikon A1 Confocal Microscope System. For flow cytometry analyses, 50 nM Cy5 labeled NPs were incubated with MDA-MB-231 cells for 1, 3, 6, 12 and 24 h. After that, the cells were washed and analyzed by a Cytoflex flow cytometer (Beckman).

Specific binding in mixture system *in vitro*

To evaluate the specific binding of NPs *in vitro*, Dio pre-staining MDA-MB-231 cells were mixed with the same amount of normal mammary epithelial cells (MCF10A and 184B5) or control tumor cells (MDA-MB-453) with slightly rotating. And then, 50 nM Cy5-conjugated NPs was added to the mixture and further incubated at 37 ^{o}C for 2 h. After that, the mixture was collected and analyzed by flow cytometer. The binding efficiency was calculated using the following formula:

Binding efficiency = ratio of Cy5 positive MDA-MB-231 cells/ratio of total MDA-MB-231 cells in mixture ×100%. The NPs binding efficiency was also represented by the value of MFI of Cy5 positive cells.

Cell viability, cell cycle and apoptosis assays

MDA-MB-231 cells were treated with 50 nM pRNA-EGFRapt-siXBP1 NPs or pRNA-EGFRapt-siScramble control. The cells viability, cell cycle and apoptosis were analyzed after three days culture. Cell viability was measured using the CCK8 assay (Dojindo), following the manufacturers protocol. In a dox sensitivity experiment, MDA-MB-231 cells were treated with dox (2 μg/mL, 0.5 μg/mL and 0.25 μg/mL, respectively) alone, or plus 50 nM NPs for 72 h. Follow that, the cell viability was measured using the same method. To analyze cell cycle, cells were incubated with NPs for 72 h. After that, cell pellets were collected, permeabilized with 70% (v/v) ethanol, and re-suspended in 1 mL of PBS containing 1 mg/mL RNase and 50 mg/mL propidium iodide (PI), incubated in the dark for 30 min at room temperature, and analyzed by a Cytoflex Flow Cytometer (Beckman). The cell cycle distribution was evaluated on DNA plots using a MODFIT software. To test apoptosis, annexin V and 7AAD staining (Southern biotech) was performed by flow cytometry.

Colony formation assay

The soft agar colony formation assay was performed as described previously with some modifications [31]. 1×10^3 pRNA-EGFRapt-siXBP1 NPs treated breast cancer cells were transferred to 0.8 % agarose with the same volume ratio (1:1) in 10% growth medium to make a final concentration of 0.4 % agarose. The cell mixture was plated on top of 0.8 % bottom layer of agar in the 10% growth medium in 6-well plates. Cells were fed every 5 days for 20 days with 10% growth medium containing 0.4 % agarose. For the dox sensitivity experiment, the breast cancer cells were firstly treated with 0.01 μg/mL dox alone, or dox plus prepared NPs for 48 h. After that the treated breast cancer cells were mixed with 0.4% agarose and seeded to the top of a solidified layer for further incubation. The experiment was repeated three times and the statistical significance was calculated using Student's t test.

Real-Time PCR

Total RNA was extracted from cultured cells or tumor tissues using a RNeasy mini kit (Qiagen), and reverse-transcription was performed by using HiScript II QRT SuperMix for qPCR (Vazyme Bioteche). Real-time PCR was performed as described previously [4].

Western blotting

Cells were lysed using RIPA buffer (CST) supplemented with cocktail protease inhibitors (Roche) and PMSF. Minced tumor tissues were homogenized in liquid nitrogen in RIPA buffer. 30 μg of total protein were separated by SDS-PAGE and the separated protein were transferred to PVDF membranes (Millipore) for western blotting analysis using anti-XBP1 (Abcam, ab37152); anti-β-actin (CST).

Orthotopic Xenograft Breast Tumor Mouse Model

Six-week-old female athymic nude mice were purchased from Beijing Vital River Laboratory Animal Technology, and all animal procedures were performed under IACUC-approved protocols at the Zhejiang

Chinese Medical University. Athymic nude mice were orthotopically injected with 1×10^7 MDA-MB-231 cells mixed with Matrigel into the fat pads of the fourth pair of mammary glands. When the tumor sizes reached 100-150 mm^3, the mice were randomly divided into five groups (six/group) and *i.v.* injected with pRNAs (3.3 nmol/mice) twice a week for 3 weeks. For dox treatments, dox (Sigma) (3 mg/kg) was intravenously injected into mice twice a week for 3 weeks and 1 day before pRNA injection. When the tumor sizes reached 1000 mm^3 (that is 25 d post-injection in this study), mice were sacrificed, and the tumors were collected and lysed for extraction of total proteins and RNAs, or fixed in 10% neutral buffered formalin, respectively, for further Western blot, real-time PCR and IHC studies, etc. The tumor volume was measured, and tumor size was calculated using the formula: volume = $0.5 \times (\text{width})^2 \times (\text{length})$.

Histochemical analysis

To examine the biodistribution of NPs within the tumor issues, O.C.T.-embedded frozen sections (5 μm) were examined by confocal microscopy. To analyze tumor cell blood vessel, the tumor tissue samples were collected and fixed in 10% neutral buffered formalin, followed by dehydration by gradient series of ethanol (75%, 85%, 95% and 100%) and embedded in paraffin following routine methods. For CD31 immunostaining, slides were blocked with 3% H_2O_2-methanol for 15 min at room temperature, treated with mouse anti-CD31 antibody (Abcam, ab28364) overnight at 4 °C, with horseradish peroxidase (HRP)-conjugated secondary antibody, and with 3, 3'-diaminobenzidine (DAB). The tissue sections were counterstained with hematoxylin for nucleus visualization. The slides were analyzed on an LSM 510 Meta confocal microscope.

Results And Discussion

Synthesis and characterization of pRNA-EGFRapt-siXBP1 NPs.

Throughout the remainder of the text, these NPs are denoted pRNA-EGFRapt-siXBP1.Our NPs harboring 2'-F modified EGFR RNA aptamer and therapeutic siXBP1, using Cy5 fluorophore as marker, were composed of four short fragments (Figure 1a). The RNA oligonucleotides were synthesized chemically (Genscript) then mixed in an equal molar ratio in TMS buffer and annealed to generate uniform NPs. 8% Native PAGE gel assays show highly effective stepwise assembly of the complex (Figure 1b), which in line with AFM result (Figure 1c). The stability assay of 2'-F-modified NPs were evaluated in 10% FBS and different concentrations RNase by naive PAGE gel assay. Compare to unmodified NPs, 2'-F-modified NPs can resistant to 100 μg/mL RNase and were stable in 10% FBS (Figure 1d) .Besides chemical modification, other NPs packaging (such as iron oxide magnetic-based NPs) can also impart higher resistance to serum and RNase to increase RNA stability [32, 33]. NPs with high thermodynamic stability prevent dissociation at ultra-low concentrations *in vivo*. The Tm value of our NPs is 68.2 ^oC (Figure 1e) determined by the LightCycler® 96 Real-Time PCR System (Roche), which means a higher stability of RNA duplex [34]. The average hydrodynamic diameter of NPs was 10.93 nm (Figure 1f). This size is larger than renal depletion cutoff sizes, while small enough to minimize macrophage phagocytosis. This size allows NPs penetrate into tumor tissues via the EPR effect and receptor-mediated endocytosis when

targeting ligands are equipped [35]. RNA NPs are indeed highly negatively charged, and this is reflected in the zeta potential measurements showing a single peak at -23.57 mV for NPs (Figure 1g).

pRNA-EGFRapt-siXBP1 NPs efficiently and specifically target and bind to TNBC cells *in vitro*.

Compare with other subtypes of the breast cancer, TNBC is overexpress EGFR protein, thus making it a potential target for TNBC targeted therapy [36]. Aptamers, often termed 'chemical antibodies', are functionally equal to protein antibodies, but with more advantages, such as ease of chemo synthesis and modification, high stability and hardly any immunogenicity. They not only can block cell surface receptors but can also deliver therapeutic agents into cells [37]. Here, we assemble NPs with EGFR aptamer, and we evaluated NPs binding efficiency by flow cytometry. The overlay histogram (Figure 2a) and median fluorescence intensity (MFI) (Figure 2b) results indicate that pRNA-EGFRapt-siXBP1 NPs efficiently bind to MDA-MB-231 cells. Confocal microscopy images further confirmed the efficient binding and internalization of pRNA-EGFRapt-siXBP1 NPs into target cells after 24 h incubation (Figure 2c).

To further confirm the binding specificity *in vitro* and mimic NPs binding to tumor cells in the presence of normal mammary epithelial cell *in vivo*, Dio pre-staining MDA-MB-231 cells were mix with MCF10A,184B5, and MDA-MB-453 cells, respectively. Flow cytometry was used to evaluate the specific binding ability of pRNA-EGFRapt-siXBP1 NPs to MDA-MB-231 cells in the mixture system (Figure 2d, 2e). The ratio of Cy5 positive MDA-MB-231 cells to total MDA-MB-231 cells and MFI in MAD-MB-231 cells was significantly higher than that of non-target cells (Figure 2f, 2g) (p<0.05). These results indicate pRNA-EGFRapt-siXBP1 NPs specifically binding ability *in vitro* and imply its specifically binding ability *in vivo*.

XBP1 gene knockdown sensitizes MDA-MB-231 cells to doxorubicin treatment *in vitro*, reduces cell viability, impairs mammospheres forming ability, but not alters cell apoptosis and cell cycle.

Our cell-binding results imply NPs could efficiently silence XBP1 expression. To verify this speculation, we firstly evaluated XBP1 mRNA and protein expression in NPs threated MDA-MB-231 cells. XBP1 mRNA expression is reduced by 80% after 50 nM pRNA-EGFRapt-siXBP1 treatment for 72 h (Figure 3a). In line with the XBP1 mRNA level decrease, XBP1 proteins expressions were also decreased (Figure 3b). It should observe that in TNBC, the effect of XBP1 silencing on cell cycle is still no studied. Our previous data showed that XBP1 knock-down in HER2+ breast cancer cell lines results in cell cycle arrest in S phase [4]. Here, we firstly show that XBP1 silencing in TNBC cannot induce cell cycle alternation (Figure 3c). Cell cycle alternation trigger cell death pathways [38]. We further measured cell apoptosis changes after XBP1 silencing by an Annexin V and 7AAD assay (Figure 3d). Different with HER2+ breast cancer, the result suggests XBP1 silencing do not alter cell apoptosis (Figure 3d) [4]. As XBP1 knockdown has recently been reported to sensitize TNBC to doxorubicin (dox) treatment by siRNA interference [5], we next examined if our NPs treatment could sensitize TNBC to dox treatment *in vitro*. We found that treatment with NPs alone could slightly reduce cell viability decrease in MDA-MB-231 cells (Figure 3e). pRNA-EGFRapt-siXBP1 NPs and dox combined treatment could significantly reduce cell viability than dox treatment alone (Figure 3e). We next tested the effect of pRNA-EGFRapt-siXBP1 NPs on soft agar colony forming of MDA-MB-231 cells. Compared to pRNA-EGFRapt-siScramble control and mock group, pRNA-

EGFRapt-siXBP1 NPs pretreatment highly impaired soft agar colony forming ability of HER2+ breast cancer cells (p<0.01) (Figure 3f). Notably, dox treatment can completely abolish MDA-MB-231 cells colony forming capacity (Figure 3f). These results indicated that combined utilization of pRNA-EGFRapt-siXBP1 NPs could sensitize the TNBC to dox treatment *in vitro*.

pRNA-EGFRapt-siXBP1 NPs specifically bind to tumor cells and efficiently silence XBP1 expression *in vivo*.

Recent cancer treatments have been developed, many are often nonspecific and have toxic side effects on non-targeted tissues. To overcome these challenges, a drug needs an ideal pharmacokinetic (PK) profile to reach targeted cells specifically with little or no accumulation in healthy organs [39]. The plasma concentration-time plot of pRNA NPs shows a typical two-phase kinetics with an initial rapid distribution phase and a highly prolonged half-life (Figure 4a). This is consistent with Abdelmawl's study [40]. To analyze gene silencing capacity *in vivo*, MDAMB-231 cells were grown subcutaneously in BALB/c immuno-deficient mice. Compared to siScramble treated mice, pRNA-EGFRapt-siXBP1 NPs treatment significantly down-regulated XBP1 expression in both mRNA (Figure 4b) and protein (Figure 4c) level *in vivo*. To confirm pRNA specific binding to tumor *in vivo*, we construct a pRNA without EGFR aptamer and test its binding *in vivo*. To do this, pRNA-EGFRapt-siXBP1 NPs or control pRNA NPs were injected via the tail vein. The tissue distribution image demonstrated that Cy5-conjugated pRNA-EGFRapt-siXBP1 NPs but not control pRNA NPs without EGFR aptamer were highly accumulated in the area of the xenograft tumor after systemic administration (Figure 4d). Importantly, confocal microscopic analyses of frozen tumor sections indicated that pRNA-EGFRapt-siXBP1 NPs effectively penetrated the tumor cells but not control pRNA NPs (Figure 4e). Various positively charged macromolecules were proven to be effective in siRNA transfection. However, these poly-cations are not suitable for systemic targeted (non-liver) delivery *in vivo*; this has been a long-standing problem [41]. Here, we demonstrated pRNA NPs without poly-cations materials can specifically bind to tumor cells and efficiently silence XBP1 expression *in vivo*, which shows huge potential for *in vivo* utilization of siRNA.

Inhibition of TNBC growth, impaired angiogenesis, and sensitize them to dox by combination treatment with pRNA-EGFRapt-siXBP1 NPs *in vivo*.

To analyze if XBP1 gene silencing *in vivo e*ffect TNBC growth and chemoresistance, MDA-MB-231-beaing mice were treated with pRNA-EGFRapt-siXBP1 NPs or pRNA-EGFRapt-siXBP1 NPs plus dox. Excitingly, tumor growth of TNBC tumors was significantly inhibited by pRNA-EGFRapt-siXBP1 NPs (*p<0.05*) (Figure 5a). Strikingly, the tumor volume was further reduced significantly after pRNA-EGFRapt-siXBP1 plus dox treatment as compared to dox treatment alone group (p<0.05) (Figure 5a). It was reported that XBP1 can function via growth factor signaling pathways to regulate endothelial proliferation and angiogenesis [42]. Here, we investigated the relationship between XBP1 expression and angiogenesis in TNBC mouse model. Our tumor frozen sections were stained with CD31 antibody and blood vessels area was counted by ImageJ software (Figure 5b). We confirmed that XBP1 depletion by pRNA-EGFRapt-siXBP1 NPs in TNBC impaired angiogenesis (Figure 5C) (p<0.05). Although decreased angiogenesis was observed in

dox only treated mice, no significant difference was observed. Notably, the blood vessels area was further reduced after pRNA-EGFRapt-siXBP1 NPs plus dox treatment than pRNA-EGFRapt-siScr NPs plus dox group (Figure 5c) (p<0.05). It was reported that XBP1 promotes TNBC by regulating the HIF1α pathway [5]. When studying the HIF1α target expressions of pRNA-EGFRapt-siXBP1 plus dox treated MDA-MB-231 tumor, we observed that combined treatment highly down-regulated HIF1α targets *VEGFA, PDK1, DDIT4* and GLUT1 expression than dox alone treated mice (Figure 5d) (p<0.001).

Conclusions

In conclusion, we assembled RNase resistant macromolecular RNA NPs equipped with EGFR targeting aptamer and therapeutic macromolecular siRNA drug to sensitize TNBC to chemotherapy utilizing bacteriophage phi29 derived pRNA. Intravenous injections of RNA NPs with EGFR aptamer result in strongly bounding to tumors and XBP1 silencing *in vivo*. XBP1 deletion by RNA NPs impaired angiogenesis and dramatically suppressed breast cancer. Importantly, RNA NPs treatment sensitizes TNBC to chemotherapy. We believe that the macromolecular RNA NPs serves as an effective and promising platform for similarly macromolecular siRNA therapeutics delivery. The combination of macromolecular RNA NPs and siRNA can likely be utilized to open new possibilities for targeted and specific treatment of breast cancer and other malignancies.

Abbreviations

TNBC: triple-negative breast cancer; XBP1: X-box-binding protein 1; NP: nanoparticles; EGFR: epidermal growth factor receptor; OS: overall survival; HER2: human epidermal growth factor receptor 2; NAC: neoadjuvant chemotherapy; dox: doxorubicin; MFI: median fluorescence intensity; PK: pharmacokinetic.

Declarations

Ethics approval and consent to participate

All animal procedures were performed under IACUC-approved protocols at the Zhejiang Chinese Medical University.

Consent for publication

All authors have agreed to publish this article..

Competing interests

The authors declare that they have no competing interests.

Funding

This work was supported by the National Natural Science Foundation of China (31800833, 21977081, 81601626 and 81703713), Zhejiang Provincial Natural Science of Foundation of China (LZ19H180001 and Y20C070010), Wenzhou Medical University and Wenzhou Institute, University of Chinese Academy of Sciences (WIBEZD2017001-03, WIUCASQD2019002 and WIUCASYJ2020001-5).

Availability of data and materials

All data generated or analyzed during this study are included in this article.

Author contributions

Zhang L, Li H, Zhang T and Shen J designed experiments; Zhang L conceived and performed the experiments. Mu C, Fan L, and Liu C performed MDA-MB-231 cancer mouse tumorigenicity assay, intravenously injection and tumor measurement. Zhang T and Zhang L performed living imaging studies. Zhang T, Yang D, Wang C, and Chen Q performed confocal studies. Zhang L, Mu C and Zhang T wrote the manuscript. Li H, Zhang T and Shen J commented on the manuscript. Li H and Chen H provided funding for this project. Li H and Shen J supervised experiments. All authors edited and approved the final manuscript.

Acknowledgements

Not applicable.

References

1. Foulkes WD, Smith IE, Reis-Filho JS. Triple-negative breast cancer. N Engl J Med, 2010, 363: 1938-1948
2. Kim C, Gao R, Sei E*, et al.* Chemoresistance evolution in triple-negative breast cancer delineated by single-cell sequencing. Cell, 2018, 173: 879-893 e813
3. Zhang J, Zhang Y, Tang S*, et al.* Evaluation bias in objective response rate and disease control rate between blinded independent central review and local assessment: A study-level pooled analysis of phase iii randomized control trials in the past seven years. Ann Transl Med, 2017, 5: 481
4. Zhang L, Mu C, Zhang T*, et al.* Systemic delivery of aptamer-conjugated xbp1 sirna nanoparticles for efficient suppression of her2+ breast cancer. ACS Appl Mater Interfaces, 2020,
5. Chen X, Iliopoulos D, Zhang Q*, et al.* Xbp1 promotes triple-negative breast cancer by controlling the hif1alpha pathway. Nature, 2014, 508: 103-107
6. Gomez BP, Riggins RB, Shajahan AN*, et al.* Human x-box binding protein-1 confers both estrogen independence and antiestrogen resistance in breast cancer cell lines. FASEB J, 2007, 21: 4013-4027
7. Zhao N, Cao J, Xu L*, et al.* Pharmacological targeting of myc-regulated ire1/xbp1 pathway suppresses myc-driven breast cancer. J Clin Invest, 2018, 128: 1283-1299

8. Goel V, Gosselin NH, Jomphe C*, et al.* Population pharmacokinetic-pharmacodynamic model of serum transthyretin following patisiran administration. Nucleic Acid Ther, 2020,
9. de Fougerolles A, Vornlocher HP, Maraganore J*, et al.* Interfering with disease: A progress report on sirna-based therapeutics. Nat Rev Drug Discov, 2007, 6: 443-453
10. Chauhan AS. Dendrimers for drug delivery. Molecules, 2018, 23:
11. Pi F, Binzel DW, Lee TJ*, et al.* Nanoparticle orientation to control rna loading and ligand display on extracellular vesicles for cancer regression. Nat Nanotechnol, 2018, 13: 82-89
12. Zhang Y, Zhang Y, Guo Q*, et al.* Trained macrophage bioreactor for penetrating delivery of fused antitumor protein. ACS Appl Mater Interfaces, 2019, 11: 23018-23025
13. Wang P, Zhang L, Zheng W*, et al.* Thermo-triggered release of crispr-cas9 system by lipid-encapsulated gold nanoparticles for tumor therapy. Angew Chem Int Ed Engl, 2018, 57: 1491-1496
14. Song Q, Yin Y, Shang L*, et al.* Tumor microenvironment responsive nanogel for the combinatorial antitumor effect of chemotherapy and immunotherapy. Nano Lett, 2017, 17: 6366-6375
15. Wolfrum C, Shi S, Jayaprakash KN*, et al.* Mechanisms and optimization of in vivo delivery of lipophilic sirnas. Nat Biotechnol, 2007, 25: 1149-1157
16. Chitkara D, Singh S, Mittal A. Nanocarrier-based co-delivery of small molecules and sirna/mirna for treatment of cancer. Ther Deliv, 2016, 7: 245-255
17. Whitehead KA, Langer R, Anderson DG. Knocking down barriers: Advances in sirna delivery. Nat Rev Drug Discov, 2009, 8: 129-138
18. Guo P, Zhang C, Chen C*, et al.* Inter-rna interaction of phage phi29 prna to form a hexameric complex for viral DNA transportation. Mol Cell, 1998, 2: 149-155
19. Shu D, Shu Y, Haque F*, et al.* Thermodynamically stable rna three-way junction for constructing multifunctional nanoparticles for delivery of therapeutics. Nat Nanotechnol, 2011, 6: 658-667
20. Guo S, Vieweger M, Zhang K*, et al.* Ultra-thermostable rna nanoparticles for solubilizing and high-yield loading of paclitaxel for breast cancer therapy. Nat Commun, 2020, 11: 972
21. Jasinski D, Haque F, Binzel DW*, et al.* Advancement of the emerging field of rna nanotechnology. ACS Nano, 2017, 11: 1142-1164
22. Peer D, Karp JM, Hong S*, et al.* Nanocarriers as an emerging platform for cancer therapy. Nat Nanotechnol, 2007, 2: 751-760
23. Miller MA, Mikula H, Luthria G*, et al.* Modular nanoparticulate prodrug design enables efficient treatment of solid tumors using bioorthogonal activation. ACS Nano, 2018, 12: 12814-12826
24. Xu C, Haque F, Jasinski DL*, et al.* Favorable biodistribution, specific targeting and conditional endosomal escape of rna nanoparticles in cancer therapy. Cancer Lett, 2018, 414: 57-70
25. Li H, Zhang K, Pi F*, et al.* Controllable self-assembly of rna tetrahedrons with precise shape and size for cancer targeting. Adv Mater, 2016, 28: 7501-7507
26. Haque F, Pi F, Zhao Z*, et al.* Rna versatility, flexibility, and thermostability for practice in rna nanotechnology and biomedical applications. Wiley Interdiscip Rev RNA, 2018, 9:

27. Liu J, Guo S, Cinier M*, et al.* Fabrication of stable and rnase-resistant rna nanoparticles active in gearing the nanomotors for viral DNA packaging. ACS Nano, 2011, 5: 237-246
28. Guo S, Li H, Ma M*, et al.* Size, shape, and sequence-dependent immunogenicity of rna nanoparticles. Mol Ther Nucleic Acids, 2017, 9: 399-408
29. Shu Y, Shu D, Haque F*, et al.* Fabrication of prna nanoparticles to deliver therapeutic rnas and bioactive compounds into tumor cells. Nat Protoc, 2013, 8: 1635-1659
30. Esposito CL, Passaro D, Longobardo I*, et al.* A neutralizing rna aptamer against egfr causes selective apoptotic cell death. PLoS One, 2011, 6: e24071
31. Horibata S, Vo TV, Subramanian V*, et al.* Utilization of the soft agar colony formation assay to identify inhibitors of tumorigenicity in breast cancer cells. J Vis Exp, 2015, e52727
32. Draz MS, Fang BA, Zhang P*, et al.* Nanoparticle-mediated systemic delivery of sirna for treatment of cancers and viral infections. Theranostics, 2014, 4: 872-892
33. Yang Z, Duan J, Wang J*, et al.* Superparamagnetic iron oxide nanoparticles modified with polyethylenimine and galactose for sirna targeted delivery in hepatocellular carcinoma therapy. Int J Nanomedicine, 2018, 13: 1851-1865
34. Freier SM, Kierzek R, Jaeger JA*, et al.* Improved free-energy parameters for predictions of rna duplex stability. Proc Natl Acad Sci U S A, 1986, 83: 9373-9377
35. He C, Liu D, Lin W. Self-assembled core-shell nanoparticles for combined chemotherapy and photodynamic therapy of resistant head and neck cancers. ACS Nano, 2015, 9: 991-1003
36. Hossein-Nejad-Ariani H, Althagafi E, Kaur K. Small peptide ligands for targeting egfr in triple negative breast cancer cells. Sci Rep, 2019, 9: 2723
37. Zhou J, Rossi JJ. Cell-specific aptamer-mediated targeted drug delivery. Oligonucleotides, 2011, 21: 1-10
38. Zuazua-Villar P, Rodriguez R, Gagou ME*, et al.* DNA replication stress in chk1-depleted tumour cells triggers premature (s-phase) mitosis through inappropriate activation of aurora kinase b. Cell Death Dis, 2014, 5: e1253
39. Rosenblum D, Joshi N, Tao W*, et al.* Progress and challenges towards targeted delivery of cancer therapeutics. Nat Commun, 2018, 9: 1410
40. Abdelmawla S, Guo S, Zhang L*, et al.* Pharmacological characterization of chemically synthesized monomeric phi29 prna nanoparticles for systemic delivery. Mol Ther, 2011, 19: 1312-1322
41. Xia Y, Tian J, Chen X. Effect of surface properties on liposomal sirna delivery. Biomaterials, 2016, 79: 56-68
42. Zeng L, Xiao Q, Chen M*, et al.* Vascular endothelial cell growth-activated xbp1 splicing in endothelial cells is crucial for angiogenesis. Circulation, 2013, 127: 1712-1722

Figures

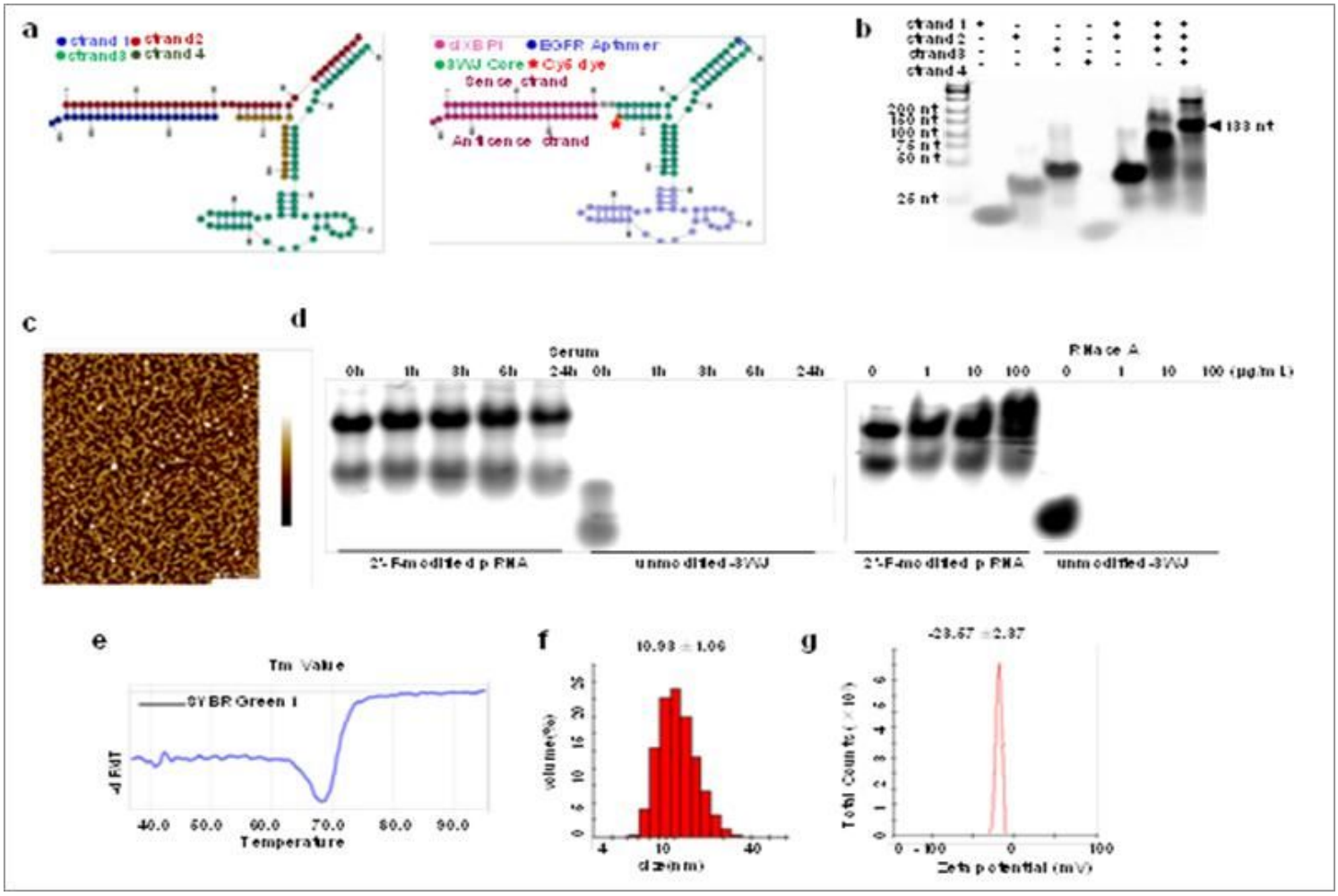

Figure 1

Characterizations of pRNA-EGFRapt-siXBP1 NPs. (a) Scheme of pRNA-EGFRapt-siXBP1NPs. (b) Native PAGE showing stepwise highly efficient assembly of the NPs. (c) Atomic force microscopy (AFM) images of pRNA nanoparticles. (d) Stability analyze by 8% native PAGE gel electrophoresis after RNase A and10% FBS-supplemented DMEM medium treatments for the indicated time at 37 °C. (e) Tm value of pRNA-EGFRapt-siXBP1 NPs determined by SYBR Green assay. (f) DLS measurements showing the hydrodynamic size. (g) Zeta potential.

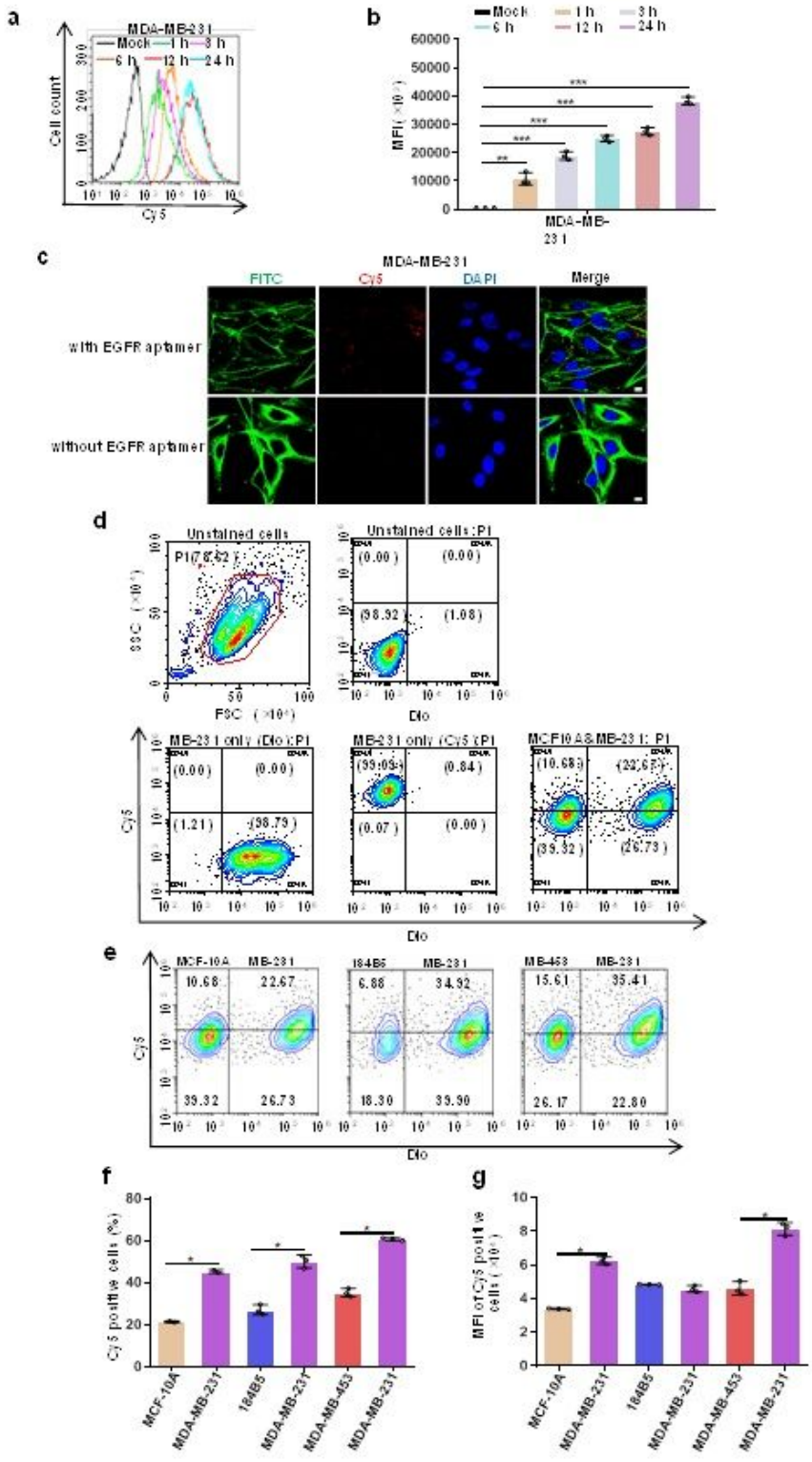

Figure 2

pRNA-EGFRapt-siXBP1 NPs cell uptake, specific binding to tumor cells in vitro. (a, b) Cell binding is assessed by flow cytometry. (c) Confocal images showing efficient binding and internalization into MDA-MB-231 cells. Green: cell membrane; blue: nuclei; and red: RNA nanoparticles. Scale bars, 10 μm. (d) Representative gating strategies in mixture of MDA-MB-231 and MCF10A cells. (e) Cell specific binding is

assessed by flow cytometry. (f) pRNA-EGFRapt-siXBP1 NPs binding efficiency were evaluated. (g) MFI of Cy5 positive cells.

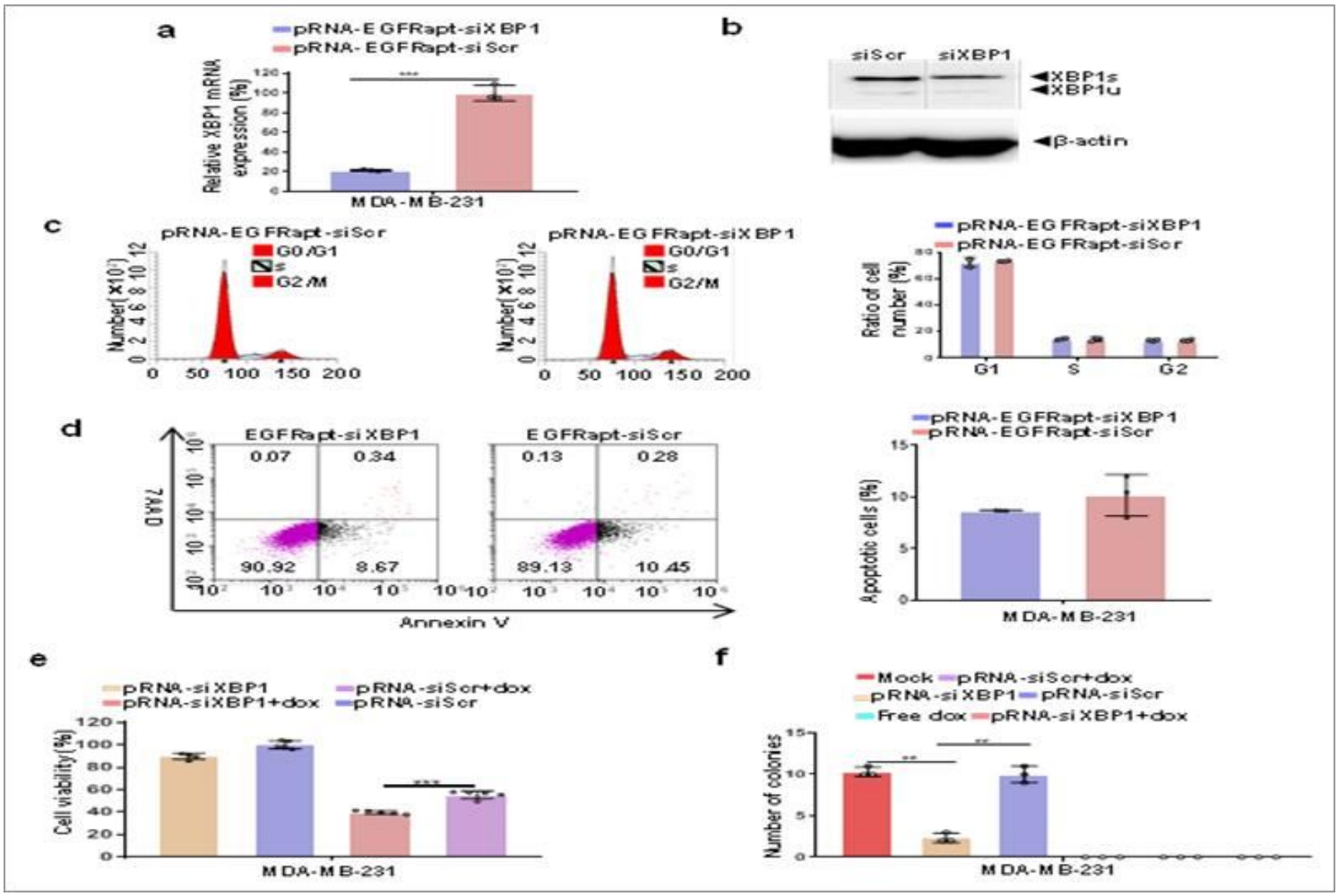

Figure 3

pRNA-EGFRapt-siXBP1 NPs silenced XBP1 expression, sensitizes MDA-MB-231 cells to doxorubicin treatment in vitro, reduces cell viability, impairs mammospheres forming ability, but not alters cell apoptosis and cell cycle. (a) RT-PCR result of XBP1 gene expression in MDA-MB-231 cells after treated with 50 nM NPs. (mean ± s.d., n = 3). ***, p<0.001. (b) Western blot analysis of XBP1s and XBP1u expression in MDA-MB-231cells after pRNA-EGFRapt-siXBP1 NPs treatment for 72 h. (c) Flow cytometry analysis of MDA-MB-231 cells cell cycle alteration after treated by pRNA-EGFRapt-siXBP1 or pRNA-EGFRapt-siScr control, respectively. (mean ± s.d., n = 3). (d) Cell apoptosis determined by annexin V and 7AAD staining. (e) Cell viability analysis of MDA-MB-231 cells after treated by NPs or NPs plus dox for 72 h. (mean ± s.d., n = 5-7). ***, p<0.001. (f) Quantification of soft agar colony formation in different groups. (mean ± s.d., n = 3). **, p<0.01. **.

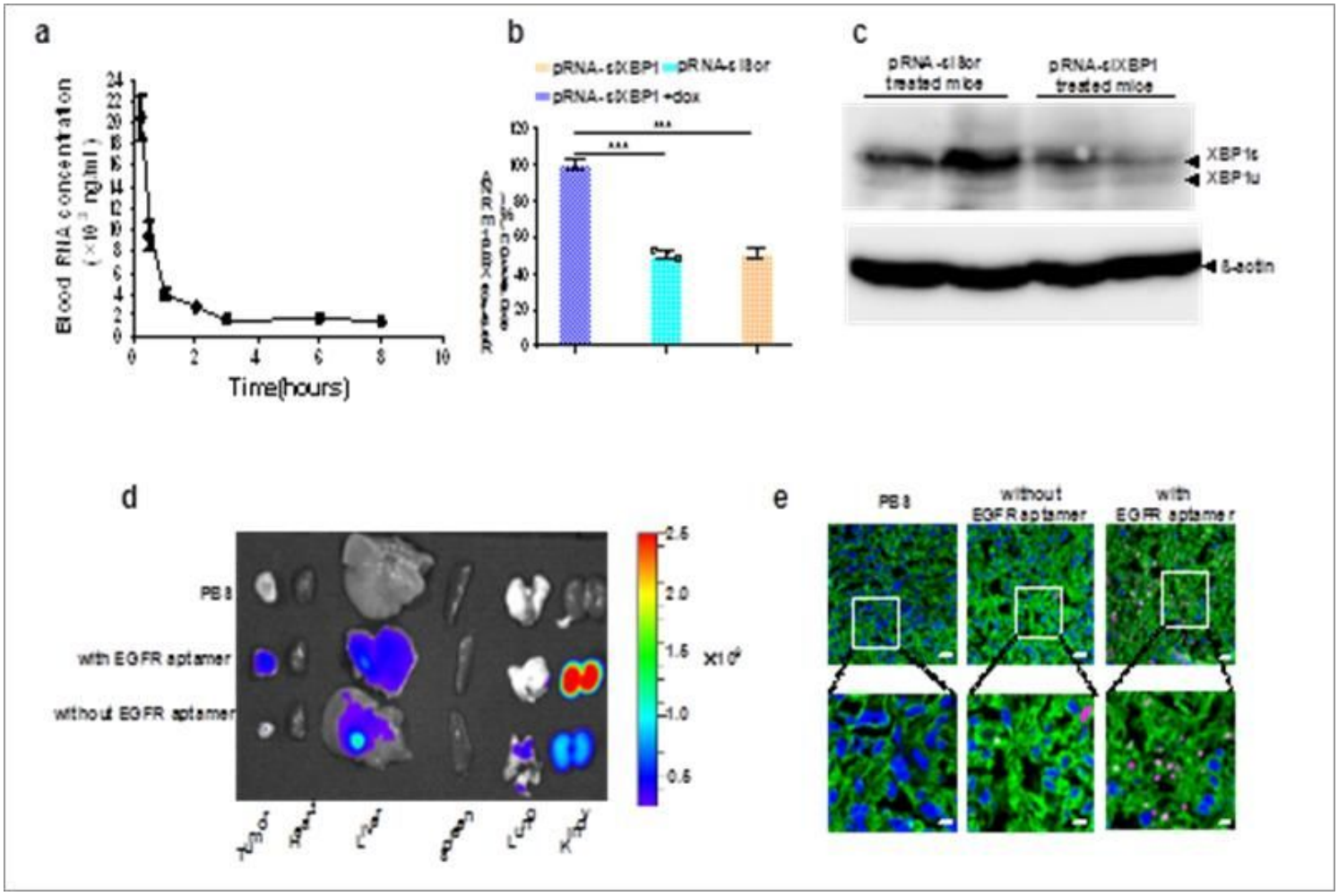

Figure 4

pRNA-EGFRapt-siXBP1 NPs specifically bind to tumor cells and efficiently silence XBP1 expression in vivo. (a) Pharmacokinetic study of pRNA-EGFRapt-siXBP1. (b) Quantitative RT-PCR analysis of XBP1 expression in MDA-MB-231 xenograft tumor. Data are presented relative to β-actin. n=3. (c) Western blot analysis of XBP1s and XBP1u expression in MDA-MB-231 tumor mouse. (d) Biodistribution of Cy5-labeled pRNA-EGFRapt-siXBP1 NPs 16 h post intravenously injection. (e) Confocal microscopic images of tumor sections from mice injected intravenously with pRNA-EGFRapt-siXBP1 or control NPs without EGFR aptamer. Red, Cy5-labelled pRNA; green, Alexa488-wheat germ agglutinin-labelled cell membrane; blue, nuclear staining with DAPI. Scale bars, 20 μm and 7 μm, respectively.

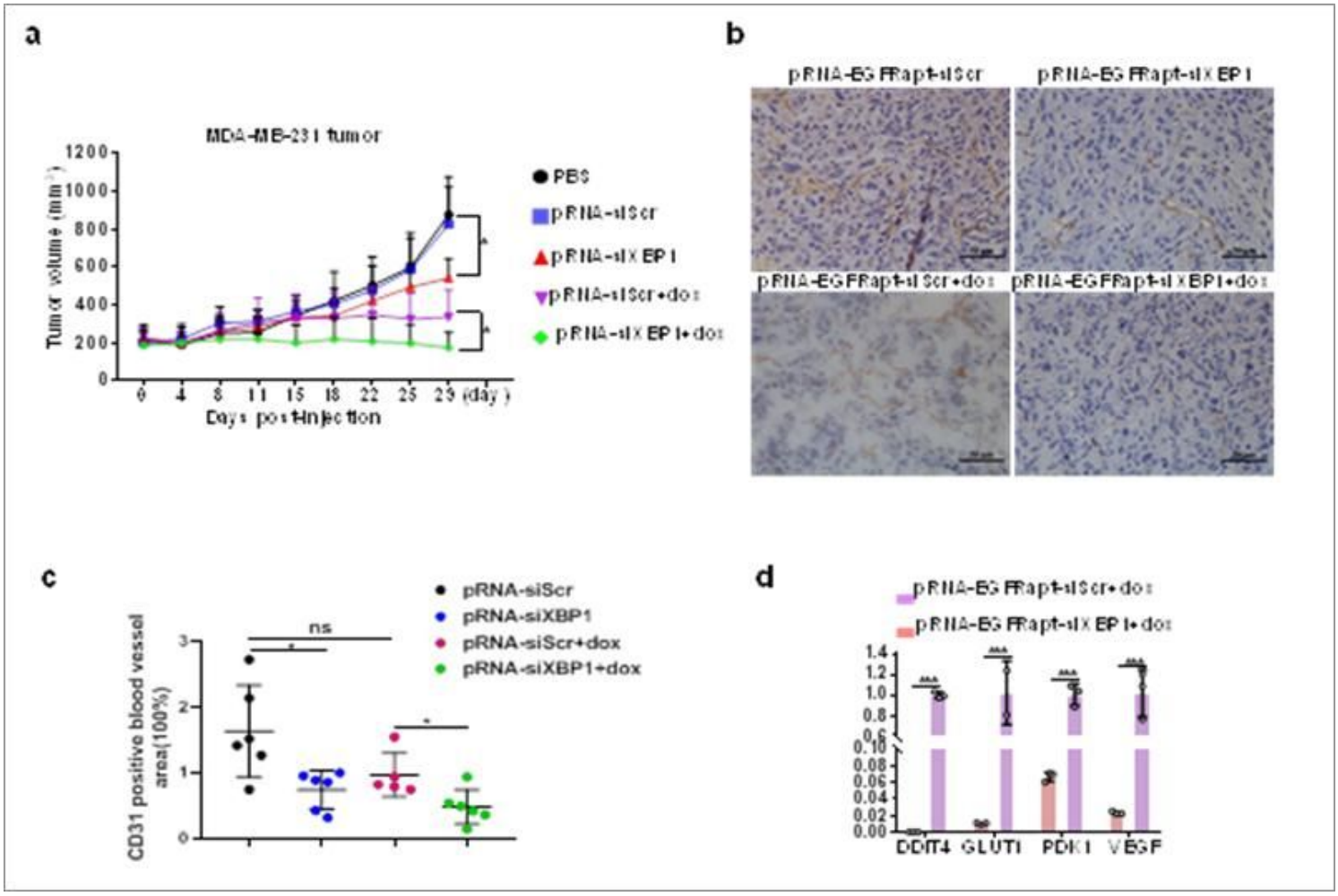

Figure 5

pRNA-EGFRapt-siXBP1 NPs treated inhibits TNBC in vivo. (a) Tumor growth in different group treated TNBC mice. (mean ± s.d., n = 5). *, p<0.05. (b, c) CD31immunostaining of TNBC tumor. Scale bars, 50 μm. (d) Quantitative RT-PCR analysis of VEGFA, PDK1, GLUT1, and DDIT4 expression in TNBC tumor after pRNA-EGFRapt-siScr plus dox and pRNA-EGFRapt-siXBP1 plus dox treatment. Results are presented relative to β-actin expression. (mean±s.d., n=5). ***, p<0.001.